Axisymmetric Rotating Flow over a Permeable Surface with Heat and Mass Transfer Effects

by

Muhammad Faraz
Reg. No. 00000321290

A thesis submitted in partial fulfillment of the requirements for the degree of

Master of Philosophy in Mathematics

Supervised by

Dr. Meraj Mustafa Hashmi

Department of Mathematics

School of Natural Sciences,

National University of Sciences and Technology,

Islamabad, Pakistan

2022

National University of Sciences & Technology

MS THESIS WORK

We hereby recommend that the dissertation prepared under our supervision by: Muhammad Faraz, Regn No. 00000321290 Titled: **"Axisymmetric Rotating Flow over a Permeable Surface with Heat and Mass Transfer Effects"** accepted in partial fulfillment of the requirements for the award of **MS** degree.

Examination Committee Members

1. Name: DR. MUHAMMAD ASIF FAROOQ   Signature: _____

2. Name: DR. MONIBA SHAMS   Signature: _____

3. Name: DR. RAI SAJJAD SAIF   Signature: _____

External Examiner: DR. ZAHID IQBAL   Signature: _____
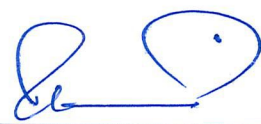
Supervisor's Name: DR. MERAJ MUSTAFA HASHMI   Signature: _____

_____
Head of Department

24/02/2022
Date

COUNTERSINGED

Date: 24.2.2022

_____
Dean/Principal

This thesis is dedicated to my loving parents and brothers.

Acknowledgments

All the appreciations and praises are for the most omnipotent **ALMIGHTY ALLAH**, the lord of the world, the most Generous and Merciful that knows the hidden truth of whatever is within and beyond the horizons of this universe.

I consider it an honor to express my heartfelt appreciation to my respected supervisor **Dr. Meraj Mustafa Hashmi** for his continued support during my research, for his patience and motivation. During the study and writing time of this thesis, he kept me well-directed and focused. I would like to express my sincere thanks to the members of my GEC, **Dr. Moniba Shamas**, **Dr. M. Asif Farooq** and **Dr. Rai Sajjad.**

This recognition will be worthless unless I give my heartfelt veneration to my loving parents over the difficult time of this research for their sacrifices, tremendous efforts, excellent contributions, financial help and motivation. During my thesis, I will extend my gratitude to my brothers for their support.

There is a humongous list of people other than my family who deserved recognition. This is the family with which I am blessed at NUST. Unfortunately, I can't list all of them here. I would like to extend my gratitude to my beloved friends **Zartab Ali** and **Furqan Nazeer** who were always there whenever I needed them, no matter what. A very special thanks to **Talat Rafiq**, **Muhammad Talha Aziz** and **Ammara Bhatti** who helped and supported me throughout my MS duration. Apart from him, this beautiful gesture is found in **Safder Hussain**, **Izaz Ahmad**, **Ali Raza Bhutto**, **Noman Ahmed**, **Safi Ur Rehman**, **Deepak Kumar**, **Sofia Sarwar**, **Humna Arshad Butt**, **Javaria Aafaq** and **Masoom Zahra** all are **NUSTIANS** and a part of me and my journey here at NUST, intangible and vital. They believed in me when, practically, no one else did. I am thankful to these special people in my life who support me, uplift me, comfort me and bring joy to my soul. I'll be very grateful for the rest of my life.

Muhammad Faraz

Table of Contents

List of Figures

List of Tables

Abstract

In this thesis, rotational flow over a permeable surface with a variable free stream angular velocity is considered in this thesis. Main interest is to solve the associated heat/mass transport equations under different situations. Firstly, heat transport phenomena occurring in generalized vortex flow is analyzed under two different heating processes, namely, the (i) prescribed surface temperature (PST) and (ii) prescribed heat flux (PHF). The vortex motion imposed at infinity is assumed to follow a power-law form $(r/r_0)^m$, where r denotes the radial coordinate, r_0 the disk radius and $m = (2n - 1)$ is a non-dimensional constant. Assuming a similarity solution, the governing Navier-Stokes equations transform into a set of coupled ordinary differential equations which are treated numerically for the aforementioned thermal conditions. Secondly, mass transport phenomena accompanied with activation energy is incorporated for the generalized vortex flow situation. After finding self-similar equations, a numerical solution is furnished by using MATLAB built-in function bvp4c.

Chapter 1

Introduction

This chapter enlightens important concepts involved in the boundary layer flows with heat/mass transfer effects. A detailed background of the research problems attempted in subsequent chapters is included. Furthermore, dimensionless number used in the thesis and their significance are explained briefly.

1.1   Incompressible and Compressible Flows

Fluid flow which exhibit density variations with respect to space variables or time are treated as compressible. Whereas, in incompressible flows, density remains constant by changing space variables or time in the incompressible flows. Liquids are treated as incompressible fluids while gases are considered as compressible fluids.

Classification of compressible and incompressible flows can be made on the basis of Mach number (which is defined as the ratio of flow velocity to the velocity of sound). If Mach number is less than 0.3, while the fluid flow is treated as compressible if Mach number is larger than 0.3.

1.2   Steady and Unsteady Flows

In steady flows, all the physical quantities (such as density, velocity, acceleration etc.) do not vary with time. Mathematically, for any quantity χ, one has:

$$\frac{\partial \chi}{\partial t} = 0, \tag{1.1}$$

For unsteady flow, physical quantities functions of time. Therefore, we have

$$\frac{\partial \chi}{\partial t} \neq 0, \tag{1.2}$$

for any physical quantity χ.

1.3 Laminar and Turbulent Flows

Laminar flow is a kind of flow in which each fluid particle follows a definite path and streamlines do not cross each other. Turbulent flow, on the other hand, does not exhibit a regular pattern of flow that leads to the rapid changes in physical properties of the fluid. For example, the flows in a pipe at low speeds and flow of water along the edges of river/lake describe laminar flows. When a dye drop is injected in water, it spreads in all possible directions without following any proper pattern, thereby making the flow turbulent.

Reynolds number determines whether the flow is turbulent/laminar. It is laminar for $Re < 2000$ and turbulent for $Re > 4000$. The laminar and turbulent flow situations for flow past a circular cylinder are illustrated in Fig. 1.1.
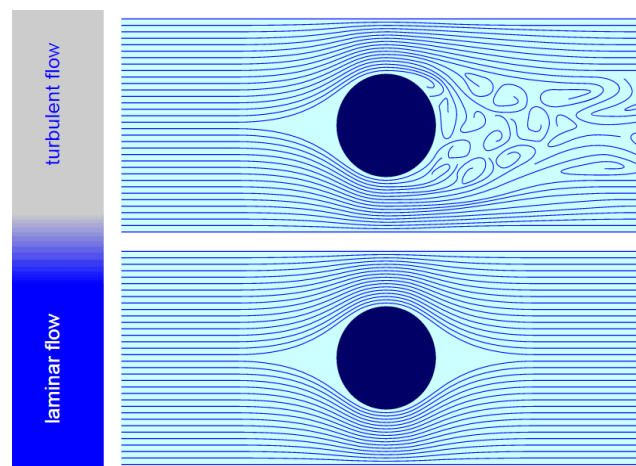
Fig. 1.1: Laminar and turbulent flow situations for flow around a circular cylinder (Source: Internet).

1.4 Continuity Equation

According to the law of conservation of mass, mass can neither be created nor be demolished but, can be transformed from one form to another. It suggests that if we consider the differential control volume system enclosed by a surface fixed in a space, then the mass inside a fixed control system will remain constant. De facto, the accumulation of mass within a control volume solely relies upon net mass inflow (by assuming zero internal forces). Mathematically, it can be translated as:

$$\frac{\partial \rho}{\partial t} + \nabla . (\rho \mathbf{v}) = \mathbf{0}, \tag{1.3}$$

where $\boldsymbol{\rho}$ designates fluid density, $\mathbf{v}$ shows velocity vector and ∇ is Nabla-operator. For an incompressible fluid, Eq. (1.6) gets assumes a simpler form:

$$\nabla . \mathbf{v} = \mathbf{0}. \tag{1.4}$$

1.5 Momentum Equation

According to the Newton's second law of motion the net force $\mathbf{F}$ acting on a fluid particle equals to the time rate of change of linear momentum. Consider a control volume with dimensions dx by dy by dz. For such control volume, Newton's second law is translated into the following form:

$$m\frac{D\mathbf{v}}{Dt} = \mathbf{F}, \tag{1.5}$$

in which D/Dt is the material derivative. The law of conservation of momentum for fluid flow is given as:

$$\rho \frac{D\mathbf{v}}{Dt} = \nabla . \tau + \rho \boldsymbol{b}, \tag{1.6}$$

where τ is the Cauchy stress tensor, $\nabla . \tau = (-\nabla P + \mu \nabla^2 \mathbf{V})$ represents surface forces in which μ denotes the dynamic viscosity and $\rho \boldsymbol{b}$ gives the net body force.

1.6 Energy Equation

The energy equation is given by the total change in energy as a result of net heat conduction and the work done by the stresses. Mathematically, the law of conservation of energy translates into the following equation:

$$\frac{D\mathrm{e}}{Dt} = -\nabla.\boldsymbol{q} + H,$$ (1.7)

where $e = \rho C_p T$ defines enthalpy, which is the amount of heat added per unit volume and $q = -\kappa\nabla T$ is the heat flux given by Fourier heat conduction law. The governing equation for conservation of energy can be written:

$$\rho C_p\left(\frac{\partial T}{\partial t} + (\mathbf{V}.\nabla)T\right) = \nabla.(\kappa\nabla T) + H.$$ (1.8)

1.7 Non Dimensionalization

The removal of dimensions from system via rescaling of variables basically is a technique to reduce the complexity and number of variables (governing the dynamics of a problem) and then grouping them into dimensionless, unit-less forms. The solution of a dimensionless equation obtained by reducing the number of independent variables of a governing equation using coordinate transformations in called a similarity solution.

It is a well-known face that the governing equations of fluid flow are extremely difficult to analyze, so we divert our attention towards transforming them in the most efficient form possible in order to increase the usefulness of the obtained solutions. This task is accomplished by non-dimensionalization of governing equation as well as boundary conditions, thereby providing lesser number of flow parameters.

Out of many, one benefit of this technique is the provision of scaling laws for the problem which helps in conversion of data from a small model to a large prototype. The non-dimensionalization

4

of the governing equations not only provides information about the underlying physical phenomena but also indicates the dominating force. For instance, the two differently scaled flows having similar geometry (a model and a prototype) satisfying the basic equations of fluid motion would only produce the same results if these flows had same values for all of the dimensionless parameter (i.e. the relative importance of the force is same).

1.8 Heat Transfer

Flow of thermal energy between physical systems is defined as heat transfer. Heat transmission is required whenever there is a temperature difference between physical systems. Heat can be transferred across systems in three ways: conduction, convection and radiation. These are defined in turn below.

1.8.1 Conduction

Conduction is the process of heat transfer due to molecular collisions. The word 'conduction' is repeatedly used for three different kinds of behavior: Heat conduction, electrical conduction and sound conduction. Fourier proposed that heat transfer rate per unit area varies directly with temperature gradient, i.e.,

$$\frac{Q}{A} = -k\frac{dT}{dx},$$
(1.9)

In the above equation, k is the constant of proportionality known as thermal conductivity with dimension $[MLT^{-3}K^{-1}]$, Q is the heat transfer rate, A is the area and dT/dx is the temperature gradient. The equation (1.9) is known as Fourier's Law.

1.8.2 Convection

Convection refers to the movement of fluid particles from the region of high thermal energy to the region of low thermal energy. In fluid dynamics, convection is the energy transfer due to bulk fluid

motion. Convective heat transfer arises between a fluid in a motion and a bounding surface. Convective heat transfer depends upon the nature of the flow. Therefore, convection has three forms: Forced convection, Natural (free) convection, Mixed convection. Heat transfer mechanism given by Newton's law of cooling as:

$$\frac{Q}{A} = h(T_s - T_f),$$ (1.10)

where, h is the heat transfer coefficient with dimension $[MT^{-3}K^{-1}]$, T_s and T_f represent the temperature of the object's surface and that of the environment, respectively.

1.8.3 Radiation

Radiation is the transfer of heat energy when it is carried by photons of light in the infrared and visible portion of electromagnetic spectrum. All bodies constantly emit thermal energy by the process of radiation. It does not require any medium for its transmission.

1.9 Mass Transfer

Mass transfer refers to the movement of chemical species from one location to another as a result of a concentration gradient. Diffusion is the same as conduction when it comes to mass transfer. Heat and mass transport are both kinetic processes that can be investigated independently or together. It is more efficient to couple heat and mass transfer equations in the case of diffusion-convection phenomena. Depending on the conditions, the nature, and the forces responsible for mass transfer, four basic types are distinguished:

- Diffusion in a quiescent medium.
- Mass transfer in laminar flow.
- Mass transfer in the turbulent flow
- Mass exchange between phases.

Mass transfer by diffusion and convection is revealed by the concentration isosurfaces. The flux through diffusion occurs perpendicular to the concentration isosurfaces, i.e., reactions may produce a flux of species consumed in the reaction to the reaction site. Because convection seeks to minimize concentration gradients along its main direction, it creates a greater separation between the concentration isosurfaces and occurs along the streamlines of the fluid flow.

In the transition to a turbulent flow, mass transfer fundamentally changes. Its vortex flow attributes result in large-scale fluid transfer. This transport usually has orders of magnitude larger rates than molecular transport, allowing for faster equalization of the concentration field and, in the case of a drug source, rapid propagation of the substance over the flow cross section.

1.10 Arrhenius Activation Energy

Arrhenius argued that for reactions to transform into products, they must first acquire a minimum amount of energy, called the activation energy. The concept of activation energy explains the exponential nature of the relationship, and in one way or another, it is present in all kinetic theories. In light of new information on the microscopic characteristics of collisional reactions, the nature of the Arrhenius activation energy and frequency factor is visited by Menzinger and Wolfgang [1].

The Arrhenius equation is a straightforward yet amazingly precise formula for determining the temperature dependence of the reaction rate constant k and hence the rate of a chemical reaction. Mathematically, the Arrhenius equation [1] is:

$$k = Ae^{-\frac{E_a}{RT}}, \tag{1.11}$$

In above equation, T represents the absolute temperature, R is the universal gas constant, E_a denotes the activation energy, A signifies the pre-exponential factor and k indicates the rate constant.

The significance of this quality that RT designates the average kinetic energy, the exponent is simply the ratio of the activation energy E_a to the average kinetic energy. The lower the rate, the higher the ratio, which is why the negative sign gets involved. This means low activation energies and high temperatures prefer a greater rate constant. As a result, these circumstances will accelerate a reaction. Because these terms occur in an exponent, their impact on the rate is significant.

1.11 Boundary Layer and Boundary Layer Thickness

When a fluid having non-zero viscosity flows past a stationary wall, the layer of the fluid that is in immediate contact with the boundary assumes the velocity of the wall. Indeed, the fluid layers are
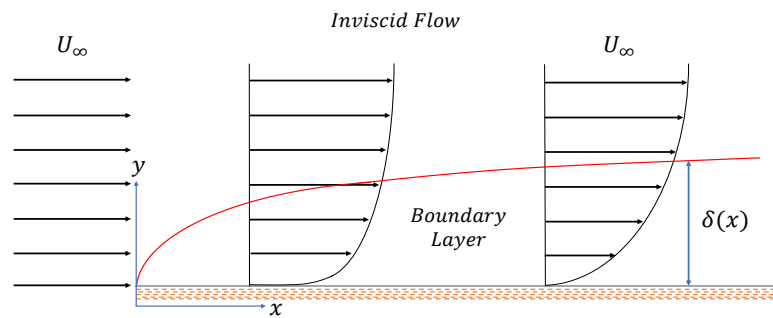
Fig. 1.2: Boundary Layer Flow.

in relative motion with the neighboring layers. Therefore, the farther we move from the wall, the lesser we feel this effect. The region of the fluid where the effect is dominant is called boundary layer.

1.12 Prandtl Number (Pr)

The Prandtl number (Pr) is used to study the relative dominance of hydrodynamic and thermal boundary layers. Mathematically, it is defined as:

$$Pr = \frac{\nu}{\alpha}, \tag{1.12}$$

where α is the thermal diffusivity and ν stands for kinematic viscosity.

1.13 Nusselt Number (Nu)

The Nusselt number Nu is a quantitative measure of convective to conductive heat transfer and it is gives to non-dimensional temperature gradient at the surface. The effect of Nusselt number to temperature boundary layer is analogous to the effect of skin friction coefficient for the velocity boundary layer. Mathematically:

$$Nu = \frac{hL}{k}, \tag{1.13}$$

where L shows the characteristic length, k gives the thermal conductivity and h represents convective heat transfer coefficient of the fluid.

1.14 Schmidt Number (Sc)

The Schmidt number (Sc) is a dimensionless number that defines the ratio of the momentum diffusivity (kinematic viscosity) to the mass diffusivity. It is used to characterize fluid flows in which momentum and mass diffusion convection processes are occurring simultaneously. Mathematically:

$$Sc = \frac{\nu}{D}. \tag{1.14}$$

1.15 Bödewadt flow

Bödewadt flow refers to the flow situation involving axisymmetric rotating flow over a plane surface. In this type of flow, fluid at infinity exhibits rigid body rotation about the vertical axis. Centrifugal force within the Bödewadt's boundary layer decreases gradually near the wall. Consequently, radial pressure gradient becomes higher than the centrifugal force thereby prompting an inward radial flow directed towards the axis of rotation. This inward radial motion triggers an upward vertical motion. This set up shows a three-dimensional flow situation described decades ago by Bödewadt [3].

Suppose that, in the cylindrical coordinate system (r, ϕ, z), disk is placed in the plane $z = 0$ while fluid occupies the region $z > 0$. Due to axisymmetric nature of the problem, variations with respect to coordinate ϕ are absent. Fluid at infinity rotates about vertical axis with constant angular velocity ω.

Keeping in view such assumptions, following set of equations describe the Bödewadt flow situation:

$$\frac{\partial u}{\partial r} + \frac{u}{r} + \frac{\partial w}{\partial z} = 0, \tag{1.15}$$

$$u\frac{\partial u}{\partial r} + w\frac{\partial u}{\partial z} - \frac{v^2}{r} = -\frac{1}{\rho}\frac{\partial p}{\partial r} + \nu\left\{\frac{\partial^2 u}{\partial r^2} + \frac{\partial}{\partial r}\left(\frac{u}{r}\right) + \frac{\partial^2 u}{\partial z^2}\right\}, \tag{1.16}$$

$$u\frac{\partial v}{\partial r} + w\frac{\partial v}{\partial z} + \frac{uv}{r} = \nu\left\{\frac{\partial^2 v}{\partial r^2} + \frac{\partial}{\partial r}\left(\frac{v}{r}\right) + \frac{\partial^2 v}{\partial z^2}\right\}, \tag{1.17}$$

$$u\frac{\partial w}{\partial r} + w\frac{\partial w}{\partial z} = -\frac{1}{\rho}\frac{\partial p}{\partial z} + \nu\left\{\frac{\partial^2 w}{\partial r^2} + \frac{1}{r}\frac{\partial w}{\partial r} + \frac{\partial^2 w}{\partial z^2}\right\}. \tag{1.18}$$

The system of boundary conditions reads:

$$u = 0, \quad v = 0, \quad w = 0 \quad \text{at} \quad z = 0,$$

$$u \to 0, \quad v = r\omega \quad \text{as} \quad z \to \infty,$$

(1.19)

At the far field, radial pressure gradient equal to centripetal force is induced and hence one can

write: $\partial p / \partial r = \rho r \omega^2$. With the similarity transformations as follows:

$$u = r\omega F(\eta),$$

$$v = r\omega G(\eta),$$

$$w = \sqrt{v\omega} H(\eta),$$

$$p = \frac{1}{2} \rho r^2 \omega^2 - \rho v \omega P(\eta),$$

(1.20)

where $\eta = z(\omega/v)^{1/2}$, is a similarity variable.

With the aid of transformations (1.20), Eqs. (1.15) − (1.17) take the following form:

$$H' + 2F = 0,$$ (1.21)

$$F'' - HF' - F^2 + G^2 - 1 = 0,$$ (1.22)

$$G'' - HG' + 2FG = 0,$$ (1.23)

Eqs. (1.21) – (1.23) are subjected to the following conditions:

$$F = 0, \quad G = 0, \quad H = 0 \quad \text{at} \quad \eta = 0,$$

$$F \to 0, \quad G \to 0 \quad \text{as} \quad \eta \to \infty,$$

(1.24)

The velocity profiles of above governing Eqs. (1.21) – (1.23) are shown in Fig. 1.3.
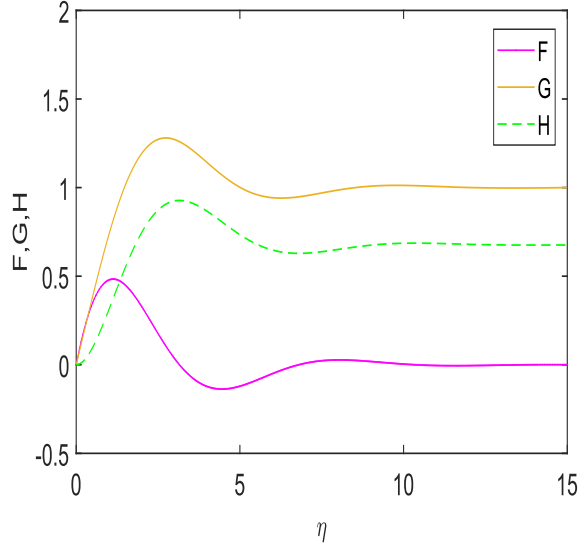
Fig. 1.3: Velocity profiles for Bödewadt flow.

1.16 Vortex Flow

For this kind of rotationally symmetric motion, the tangential velocity is assumed to satisfy a power law form, that is $v \sim r^m$, where r is radial coordinate and m is power law index. There are two special cases of vortex flow i.e. potential vortex $(m = -1)$ and rigid body rotation $(m = 1)$. In potential vortex, also known as irrotational flow, there is an inverse relation between velocity of the fluid and distance r from the vortex axis. Whereas in rigid body rotation there is direct relation of velocity and distance r from the axis of rotation. Rahman and Andersson [12] generalized the vortex flow with the heat transfer. Boundary conditions for this flow are expressed as follows:

$$u = 0, \ v = 0, \ w = v_0 \left(\frac{\nu}{v_0 r_0}\right)^{1/2} \left(\frac{r}{r_0}\right)^{n-1} (n+1) \ \text{ at } \ z = 0,$$

$$u \to 0, \ v \to v_\infty = v_0 \left(\frac{r}{r_0}\right)^{2n-1} \quad \text{ as } \ z \to \infty. \tag{1.25}$$

Using the similarity transformations:

$$u = -v_0 \left(\frac{r}{r_0}\right)^{2n-1} F(\eta), \quad v = v_0 \left(\frac{r}{r_0}\right)^{2n-1} G(\eta),$$

$$w(r,z) = v_0 \left(\frac{\nu}{v_0 r_0}\right)^{1/2} \left(\frac{r}{r_0}\right)^{n-1} [(n+1)H(\eta) + (n-1)\eta F(\eta)], \tag{1.26}$$

$$p = \frac{\rho v_0^2}{4n-2} \left(\frac{r}{r_0}\right)^{4n-2} \quad \text{with} \quad \eta = \left(\frac{z}{r_0}\right)\left(\frac{r}{r_0}\right)^{n-1} \left(\frac{v_0 r_0}{\nu}\right)^{1/2}.$$

The governing Eqs. (1.5) − (1.7) are transformed into the following ODE's:

$$H' - F = 0, \tag{1.27}$$

$$F'' - (n+1)HF' - (1-2n)F^2 - G^2 + 1 = 0, \tag{1.28}$$

$$G'' - (n+1)HG' + 2nFG = 0. \tag{1.29}$$

And the transformed boundary conditions are:

$$F = 0, \quad G = 0, \quad H = A \quad \text{at} \quad \eta = 0,$$

$$F \to 0, \quad G \to 1 \quad \text{as} \quad \eta \to \infty. \tag{1.30}$$

The results of vortex flow of velocity profiles are shown in Chapter 2 (Figs. 2.1 − 2.6).

1.17 Literature Review

Decades ago, Von-Karman [2] studied boundary layer formation above a large disk rotating with uniform angular velocity. The author demonstrated that such a problem can be dealt by using a similarity transformation. Its twin problem was later introduced by Bödewadt [3], which involves a flow situation where fluid far from an infinite plane exhibits rigid body rotation about the vertical axis (see section 1.15). Such physical phenomenon is met in a number of practical scenarios such as flow between a rotor and a stator, centrifugal pumps, viscometers, air cleaners etc. Bödewadt's work is a member of family of flows in which both ambient fluid and the disk rotate with different angular velocities. Such family of flows was introduced by Batchelor [4], where another family of flows arising between parallel plane surfaces rotating with different angular velocities is discussed.

The above referred articles led to morel findings associated with heat transfer in Bödewadt flows. Articles by Sahoo [5,6] revisited Bödewadt's analysis when a non-Newtonian fluid model was incorporated. In these papers, the associated heat transfer problem was also solved in the presence of viscos dissipation term. Turkyilmazoglu [7] came up with a concept of radial boundary stretching for Bödewadt flow and found important implications of radial wall stretching phenomena on the accompanying heat transfer. A comparative analysis of generalized non-Newtonian fluids experiencing Bödewadt flow situation, was performed by Griffiths [8], while Joshi et al. [9] employed variable viscosity assumption to analyze Bödewadt's framework under heat transfer effects. However, solution profiles computed by Joshi et al. [9] did not adhere to the asymptotic decay character, prevalent in boundary layer type flows. Later, Nath and Venkatachala [10] considered Bödewadt's work with suction and magnetic force effects.

Heat transport phenomena occurring in Bödewadt flow situation was carefully scrutinized by Rahman and Andersson [11] with the help of a closed-form solution, they figured out the importance of suction for having a meaning full solution of associated energy equation. This study also raised concerns about the reliability of numerical solutions derived by Sahoo [5], [6]. Moreover, physically acceptable solutions in Turkyilmazoglu's work [7] can be attributed to the radial stretching feature of the infinite plane surface. Later, Rahman and Andersson [12] investigated boundary layer development under a generalized vortex flow with heat transfer and elaborated the findings in terms of two different ways namely (a) variation of the effective Prandtl number that affected the thermal diffusion, and (b) an indirect variation of the axial velocity component affected the thermal convection. Heat and mass transfer, when combined with chemical reactions, has a significant impact on a variety of applications, including combustion systems, clothing dyeing, metallurgy, atomic reactor safety and chemical engineering. Almost all

chemical industries use a relatively low-cost raw material that is then processed using specially designed chemical processes to produce high-value products. In most cases, these chemical processes are based on chemical reactions that occur in the presence of heat transfer. The minimum amount of energy required to activate molecules or particles to a state where they can develop physical transportation or chemical reaction is called activation energy. The Arrhenius equation, which specifies how the rate constant changes with temperature, may be used to estimate the activation energy for a reaction. A chemical conversion and one or more products with different effects from the reactants are used to classify them.

Most living-matter operations, such as breathing, feeding, and sweating, rely on mass transfer. The mass transfer process accompanied by chemical reaction has been widely reported in the past (see [13–19] and reference therein). Because of its consequence in geothermal reservoirs, chemical engineering, nuclear reactor cooling and thermal oil retrieval, It is important to formulate a reaction that's efficient, with minimal input energy and a high yield by using sustainable methods. Bestman [20] studied the boundary layer flow involving the binary chemical reaction. Using a perturbation technique, he investigated the effects of activation energy on natural convection flow in a porous surface. Soundalgekar [21] presented an exact solution to viscous flow initiated by an impulsively started plate from rest subjected to constant heat flux and chemical reaction. Das et al. [22] elaborated mass transfer near a vertical infinite plate surface with chemical reaction. Dhlamini et al. [23] studied the combined effects of activation energy and binary chemical reaction in an unsteady mixed convective flow over a boundary of infinite length. Khan et al. [24] discussed the heat and mass transfer of an Oldroyd-B fluid flow over a rotating disk. On the energy and mass species fields, some stimulating properties such as nonlinear radiations, heat absorption/generation, and Arrhenius chemical reactions with activation energy are investigated.

15

Heat transport aspects were examined via Joule heating, thermal radiation and dissipation over a stretchable surface of disk along with chemical reaction subject to activation energy by Abbas et al. [25].

The focus of current thesis is twofold. Firstly, to solve heat transfer problem for vortex flow using two assumptions namely prescribed surface temperature (PST) and prescribed heat flux (PHF). Secondly, to address the mass transport phenomena associated with the vortex flow with flow field is equipped with chemically reactive species. In both the cases, numerical solutions are furnished to predict the contributions of embedded parameters on the underlying physical aspects.

1.18 bvp4c

Nearly all physical problems that involving rate of change encountered in the real world are coded in the language of differential equations. The analytical solutions of these differential equations are not possible every time. Therefore, attention is drifted towards solving these problems numerically using computer aided software. MATLAB is a numerical computer software of present age which is a rich in built-in ODE and PDE solvers. Most of the fluid dynamics involving nonlinear ODEs. MATLAB provides a fairly easy to implement built-in solver for such problems called bvp4c which uses an error-controlled domain discretization procedure based upon collocation method. In order to solve such a system using this package, the user is required to transforms the higher order differential equations to a first-order system and then provides the initial guess vector. The choice of initial guess vector has prime importance in finding the accurate solution of interest. Indeed, the provision of initial guess is necessary because a bvp can have multiple solutions. When it is difficult to choose an appropriate guess for a particular interval of interest, the problem is first solved on a shorter interval, generally, and after having a reasonable

choice of an initial guess, the problem is then extended to that particular interval of interest. The computations required to obtain a numerical solution is strongly based upon the choice of initial guess.

Chapter 2

A Comparative study of different Thermal Boundary Conditions for Heat Transfer in a Generalized Vortex Flow

2.1 Introduction

This chapter is based on the generalized vortex flow model investigated by Rahman and Anderson [12]. Here, development of thermal boundary layer under a generalized vortex flow is studied. A comparative study of two different thermal wall conditions for heat transfer in generalized vortex flow is presented. The cases of rigid body rotation and potential vortex corresponding to $m = 1$ and $m = -1$ are discussed.

2.2 Problem Formulation

Assume that flow is steady, three-dimensional, incompressible and laminar. The fluid motion occurs above an infinite disk residing in the plane $z = 0$ of the cylindrical coordinate system (r, φ, z). Fluid high above the disk undergoes vortex motion characterized by a power-law tangential velocity of the form $v_0 (r/r_0)^{2n-1}$. Heat transfer problem with viscous dissipation effect is dealt in two ways. Firstly, prescribed surface temperature (PST) of the form $T_w = T_\infty + T_0 (r/r_0)^{4n-2}$ is considered. Secondly, a prescribed power-law heat flux (PHF) of the form $-k\,(\partial T/\partial z) = D(r/r_0)^{5n-3}$ is incorporated. D is constant with unit W/m^2. In view of the axisymmetric flow assumption, one can ignore variations with respect to the azimuthal coordinate φ. Suppose that fluid temperature at the disk is denoted by T_w and temperature at infinite is designated by T_∞. There is no boundary layer and slip at the surface when viscosity is exactly zero. As the velocity decreases, the thickness of boundary layer approaches zero.

$$\frac{\partial}{\partial r}(ru) + \frac{\partial}{\partial z}(rw) = 0, \tag{2.1}$$

$$u\frac{\partial u}{\partial r} - \frac{v^2}{r} + w\frac{\partial u}{\partial z} = -\frac{1}{\rho}\frac{\partial p}{\partial r} + v\left(\frac{\partial^2 u}{\partial r^2} + \frac{\partial}{\partial r}\left(\frac{u}{r}\right) + \frac{\partial^2 u}{\partial z^2}\right), \tag{2.2}$$

$$\left(u\frac{\partial v}{\partial r} + \frac{uv}{r} + w\frac{\partial v}{\partial z}\right) = v\left(\frac{\partial^2 v}{\partial r^2} + \frac{\partial}{\partial r}\left(\frac{v}{r}\right) + \frac{\partial^2 v}{\partial z^2}\right), \tag{2.3}$$

$$u\frac{\partial w}{\partial r} + w\frac{\partial w}{\partial r} = -\frac{1}{\rho}\frac{\partial p}{\partial z} + v\left(\frac{\partial^2 w}{\partial r^2} + \frac{1}{r}\frac{\partial w}{\partial r} + \frac{\partial^2 w}{\partial z^2}\right), \tag{2.4}$$

$$\rho C_p\left(u\frac{\partial T}{\partial r} + w\frac{\partial T}{\partial z}\right) = k\left(\frac{\partial^2 T}{\partial r^2} + \frac{1}{r}\frac{\partial T}{\partial r} + \frac{\partial^2 T}{\partial z^2}\right) + \Phi \tag{2.5}$$

where (u, v, w) are the velocity components of the fluid radial, tangential and axial directions, respectively, and T is the temperature. The specific heat constant at constant pressure of the fluid is C_p. v is the kinetic viscosity of the fluid, k is the thermal conductivity and p is the pressure.

By means of the usual boundary layer approximations, name that $w \ll u, v$ and $\partial/\partial z \gg \partial/\partial r$, the system of Eqs. $(2.1) - (2.5)$ simplifies to:

$$\frac{\partial}{\partial r}(ru) + \frac{\partial}{\partial z}(rw) = 0, \tag{2.6}$$

$$u\frac{\partial u}{\partial r} - \frac{v^2}{r} + w\frac{\partial u}{\partial z} = -\frac{1}{\rho}\frac{\partial p}{\partial r} + v\left(\frac{\partial^2 u}{\partial z^2}\right), \tag{2.7}$$

$$\left(u\frac{\partial v}{\partial r} + \frac{uv}{r} + w\frac{\partial v}{\partial z}\right) = v\left(\frac{\partial^2 v}{\partial z^2}\right), \tag{2.8}$$

$$\frac{\partial p}{\partial z} = 0, \tag{2.9}$$

$$\rho C_p\left(u\frac{\partial T}{\partial r} + w\frac{\partial T}{\partial z}\right) = k\left(\frac{\partial^2 T}{\partial z^2}\right) + \mu\left\{\left(\frac{\partial u}{\partial z}\right)^2 + \left(\frac{\partial v}{\partial z}\right)^2\right\}, \tag{2.10}$$

For the present flow problem following boundary conditions are considered:

$$u = v = 0, \quad w = Av_0\sqrt{\frac{v}{v_0 r_0}}\left(\frac{r}{r_0}\right)^{n-1}(n+1) \qquad \text{at} \qquad z = 0,$$

$$\tag{2.11}$$

$$u = 0, \quad v = v_0\left(\frac{r}{r_0}\right)^{2n-1} \qquad \text{as} \qquad z \to \infty.$$

It is worth pointing here that pressure gradient $\partial p / \partial r$ should equal the centrifugal force per unit volume at infinity. Following is assumed for the heat transfer problem.

$$T(r,0) = T_w = T_\infty + T_0 \left(\frac{r}{r_0}\right)^{4n-2}, \qquad \textbf{(PST case)} \qquad (2.12)$$

$$-k\frac{\partial T}{\partial z}\Big|_{z=0} = D\left(\frac{r}{r_0}\right)^{5n-3}, \qquad \textbf{(PHF case)} \qquad (2.13)$$

$$\text{and} \qquad T \to T_\infty \qquad \text{as} \qquad z \to \infty, \qquad (2.14)$$

where $D = \dfrac{T_0 k \sqrt{\frac{v_0 r_0}{v}}}{r_0}$ is a constant with dimension $[\mathrm{MT}^{-3}]$ and $D > 0$.

2.3 Similarity Transformation

For transforming the governing partial differential equations (PDEs), following substitutions are made in terms of similarity variable $\eta = \left(\dfrac{z}{r_0}\right)\left(\dfrac{r}{r_0}\right)^{n-1}\sqrt{\dfrac{v_0 r_0}{v}}$.

$$u(r,z) = -v_0 \left(\frac{r}{r_0}\right)^{2n-1} F(\eta),$$

$$v(r,z) = v_0 \left(\frac{r}{r_0}\right)^{2n-1} G(\eta),$$

$$w = Av_0 \sqrt{\frac{v}{v_0 r_0}} \left(\frac{r}{r_0}\right)^{n-1} (n+1)H(\eta) + (n-1)\eta F, \qquad (2.15)$$

$$p(r) = \frac{\rho v_0}{4n-2}\left(\frac{r}{r_0}\right)^{4n-2},$$

$$T(r,z) = T_\infty + (T_w - T_\infty)\theta(\eta),$$

By using [26] $T_w - T_\infty = T_0 \left(r/r_0\right)^{4n-2}$, the similarity solution for temperature as follows:

$$T(r,z) = T_\infty + T_0 \left(\frac{r}{r_0}\right)^{4n-2} \theta(\eta), \qquad (2.16)$$

utilizing Eqs. (2.15) and (2.16) in Eqs. (2.6) − (2.10), we obtain the following ODEs:

$$H' - F = 0, \qquad (2.17)$$

20

$$F'' - (n + 1)HF' - (1 - 2n)F^2 - G^2 + 1 = 0, \tag{2.18}$$

$$G'' - (n + 1)HG' + 2nFG = 0, \tag{2.19}$$

$$\theta'' - Pr\{(n + 1) H(\eta)\theta' - (4n - 2)\theta - Ec(F'^2 + G'^2)\} = 0, \tag{2.20}$$

where $Pr = (\rho v C_p)/k$ defines the Prandtl number and $Ec = v_0^2/(C_p T_0)$ is the Eckert number.

Transformed boundary condition are given below:

$$F(\eta) = 0, \quad G(\eta) = 0, \quad H(\eta) = A \quad \text{at} \quad \eta = 0,$$
$$F(\eta) \to 0, \quad G(\eta) \to 1 \quad \text{as} \quad \eta \to \infty. \tag{2.21}$$

Boundary conditions for θ (given in Eqs. (2.11) $-$ (2.14)) are transformed as follow:

$$\theta(\eta) = 1 \quad \text{at} \quad \eta = 0, \qquad \textbf{(PST case)} \tag{2.22}$$

$$\theta'(\eta) = -1 \quad \text{at} \quad \eta = 0, \qquad \textbf{(PHF case)} \tag{2.23}$$

$$\theta(\eta) \to 0 \quad \text{as} \quad \eta \to \infty. \tag{2.24}$$

Note that the transformed system given by Eqs. (2.17) $-$ (2.20) involves the suction parameter A, the power-law parameter $n = (m + 1)/2$ and the Prandtl number Pr.

2.4 Numerical Approach

We have used the MATLAB built-in function bvp4c to solve the system consisting of Eqs. (2.17) $-$ (2.20) along with conditions (2.21) $-$ (2.24). In the bvp4c code, the equivalent first-order system is required to be inserted. To serve this purpose, we substitute:

$$(H, F, F', G, G', \theta, \theta') = (y_1, y_2, y_3, y_4, y_5, y_6, y_7),$$

which gives, from Eqs. (2.21) $-$ (2.24):

$$\begin{pmatrix} y_1' \\ y_2' \\ y_3' \\ y_4' \\ y_5' \\ y_6' \\ y_7' \end{pmatrix} = \begin{pmatrix} y_2 \\ y_3 \\ (n+1)y_1 y_3 + (1-2n)y_2^2 + y_4^2 - 1 \\ y_5 \\ (n+1)y_1 y_5 - 2n y_2 y_4 \\ y_7 \\ Pr\{(n+1)y_1 y_7 - (4n-2)y_6 - Ec(y_3{}^2 + y_5{}^2)\} \end{pmatrix}, \qquad (2.25)$$

The boundary conditions $(2.21) - (2.24)$ are transformed accordingly as:

$$\begin{pmatrix} y_1(0) \\ y_2(0) \\ y_4(0) \\ y_6(0) \\ y_2(\infty) \\ y_4(\infty) \\ y_6(\infty) \end{pmatrix} = \begin{pmatrix} A \\ 0 \\ 0 \\ 1 \\ 0 \\ 1 \\ 0 \end{pmatrix}, \qquad \textbf{(PST case)} \qquad (2.26)$$

$$\begin{pmatrix} y_1(0) \\ y_2(0) \\ y_4(0) \\ y_7(0) \\ y_2(\infty) \\ y_4(\infty) \\ y_6(\infty) \end{pmatrix} = \begin{pmatrix} A \\ 0 \\ 0 \\ -1 \\ 0 \\ 1 \\ 0 \end{pmatrix}, \qquad \textbf{(PHF case)} \qquad (2.27)$$

The set of equations given in (2.25) with the initial conditions (2.26) and (2.27) have been solved through package bvp4c. The computations have been performed in MATLAB and error tolerance of 10^{-6} is imposed. The skin friction coefficient and local Nusselt number [26] for the flow problem are defined as:

$$Re_r^{-1/2} Nu_r = -\theta'(0), \qquad (2.28)$$

$$Re_r^{1/2} C_{fr} = \{(F'(0))^2 + (G'(0))^2\}^{1/2}, \qquad (2.29)$$

where $Re_r = (v_\infty r / v)$ is the Reynolds number. The above local Nusselt number is only for PST case because in PHF case $\theta'(0) = -1$.

2.5   Results and Discussions

2.5.1 Velocity and Temperature profiles in the viscous boundary layer

In table 2.1, the radial wall shear stress $F'(0)$, azimuthal wall shear stress $G'(0)$ and volumetric

flow rate $H(\infty)$ are assessed by changing the values of parameter n in the presence of suction

parameter $A = -2.0$. The resisting wall shear is raised whenever n is gradually increased.

Theoretically speaking, suction tends to reduce momentum boundary layer thickness which in turn

elevates wall shear stresses. For increasing values of parameter n, a slight decrease in axial velocity

and volume flow rate is detected.

In table 2.2, Nusselt number data for the case of prescribed surface temperature (PST case) is given

evaluated for changing wall suction parameter A and power-law index parameter n. The power-

law fluid index, the suction parameter, Eckert number and the general linear Prandtl number are

discovered to be important in determining the solution. In table 2.2, by increasing values of suction

parameter, more heat is transferred from the solid surface for all considered values of parameter

n. Moreover, heat transfer rate from the surface is maximum in the case of higher values of n and

minimum whenever n diminishes.

Table 2.1: Boundary layer characteristic $F'(0), G'(0)$ and $H(\infty)$ with suction parameter $A = -2.0$.

n	$F'(0)$	$G'(0)$	$H(\infty)$
1.0	0.3698	4.0276	-1.9736
0.75	0.4216	3.5285	-1.9609
0.50	0.4916	3.0253	-1.9378
0.18	0.6362	2.3598	-1.8644
0.0	0.8076	1.9367	-1.7463

Table 2.2: Heat transfer rate $-\theta'(0)$ (PST case) for various values of flow behaviour index n and suction parameter A when $Pr = 7$ and $Ec = 0.5$.

$n\backslash A$	-1.0	-1.5	-2.0	-2.5
1.0	6.9466	14.0421	19.8727	25.4040
0.75	6.7605	12.6413	17.6565	22.4465
0.50	6.7518	11.3919	15.5617	19.5894
0.18	6.7324	10.0456	13.1319	16.1544
0.0	6.5604	9.3579	11.9368	14.3871

In Figs. $2.1 - 2.3$, graphs of the functions F, G and H are obtained against the similarity variable η for various choices of suction parameter A. A sharp thinning in momentum boundary layer is predicted whenever the disk is porous. In absence of suction, axial flow is upwards as in pure Bödewadt flow. For a sufficiently large value suction parameter A, the direction of axial flow becomes downward. Oscillations in all profiles seem to vanish as suction tends to infinity.

It can be concluded that in infinite suction limit, whole fluid admits rigid body rotation (as also observed by Turkyilmazoglu [7]). It is natural to witness that axial flow accelerates for increasing values of suction.

To illustrate the consequence of parameter n on the velocity components, Figs. $2.4 - 2.6$ are obtained which show plots of the functions F, G and H for different values of n. As n gradually enlarges, it takes increasingly lower distances for the profiles of F, G and H to reach their respective asymptotic values. It suggests that boundary layer thickness contracts in transition from potential vortex to pure Bödewadt situation. Axial flow at infinity is accelerated upon increasing values of n.

Temperature curves for both the imposed boundary conditions are presented in Figs. $2.7 - 2.14$. Rahman and Andersson [12] have pointed out that solution of energy equation can be meaningful only when sufficiently large value of suction parameter is selected. Figures 2.7 and 2.8 display the onset of suction on the thermal boundary layer in PST and PHF cases. A drastic thinning in thermal boundary layer is noticed for increasing values of suction parameter. Variation in temperature curves appear to be of similar magnitude in both PST and PHF cases.

Figs. 2.9 and 2.10 display the temperature curve for different choices of Prandtl number Pr in PST and PHF cases respectively. Prandtl number Pr is a dimensionless parameter used in calculations of heat transfer between a moving fluid and a solid body.

Contribution of power-law index n on the temperature profile in both PST and PHF cases is demonstrated in Figs. 2.11 and 2.12 respectively. A slight drop in temperature is noticed when n is varied from 0 to 1.

Variation in temperature profile caused by changing Eckert number Ec is noticed in Figs. 2.13 and 2.14 for PST and PHF cases respectively. Eckert number Ec gives the relative importance of heat generation as a consequence of frictional heating. Its value is higher for the cases where fluid flows at high velocity compared to the prescribed temperature difference. Physically, Eckert number measures the work done by the fluid against the viscous stresses. Graphs in the Figs. 2.13 and 2.14 indicate that thermal boundary layer expands rapidly for increasing Eckert numbers.
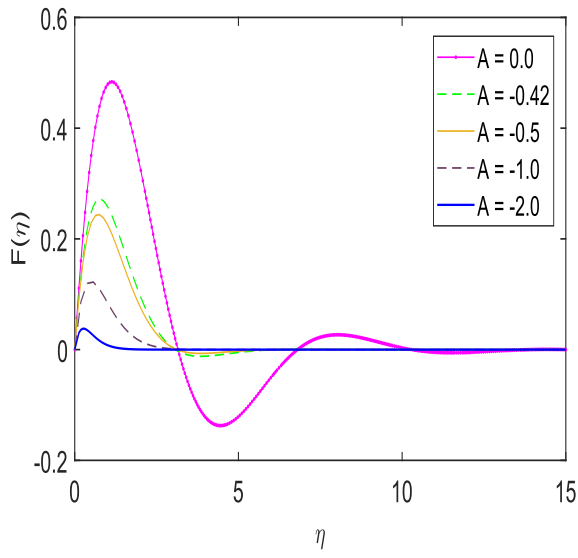
Fig. 2.1: Variation in radial velocity profile $F(\eta)$ with η for different choices of suction parameter A when $(n = 1)$.
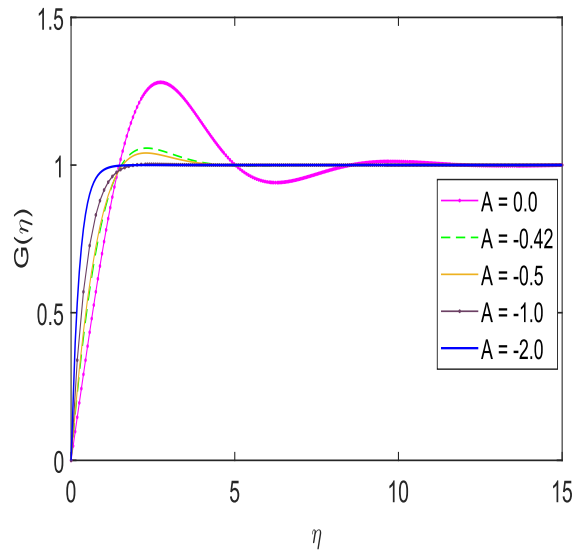
Fig. 2.2: Variation in tangential velocity profile $G(\eta)$ with η for different choices of suction parameter A when $(n = 1)$.
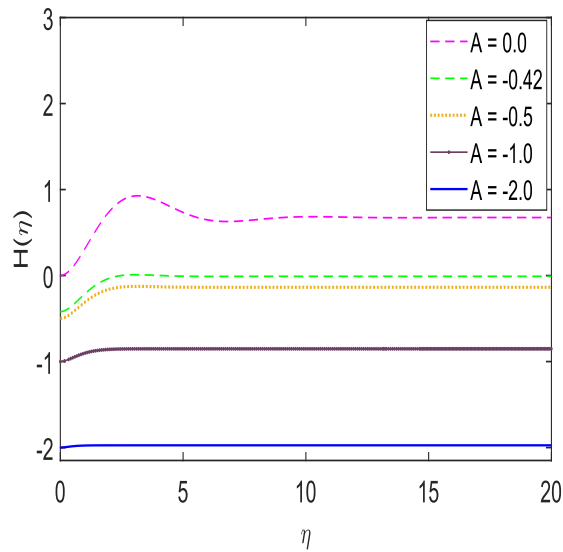
Fig. 2.3: Variation in axial velocity profile $H(\eta)$ with η for different choices of suction parameter A when $(n = 1)$.
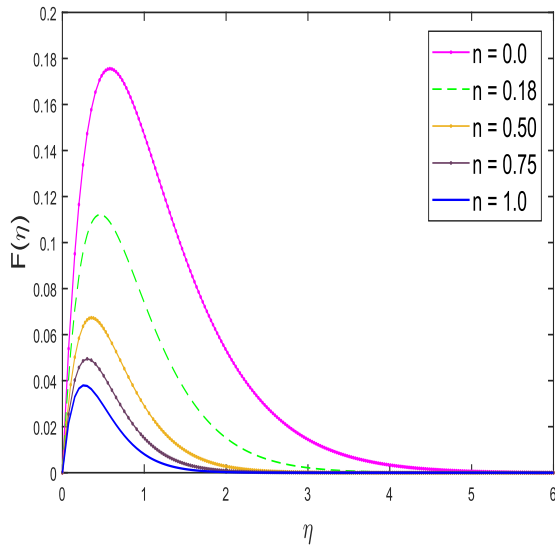
Fig 2.4: Variation in radial velocity profile $F(\eta)$ with η for different choices of power-law parameter n when $(A = -2.0)$.
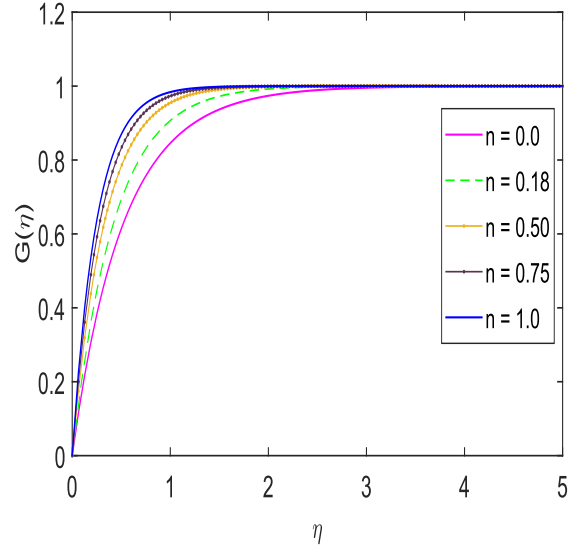
Fig. 2.5: Variation in tangential velocity profile $G(\eta)$ with η for different choices of power-law parameter n when $(A = -2.0)$.
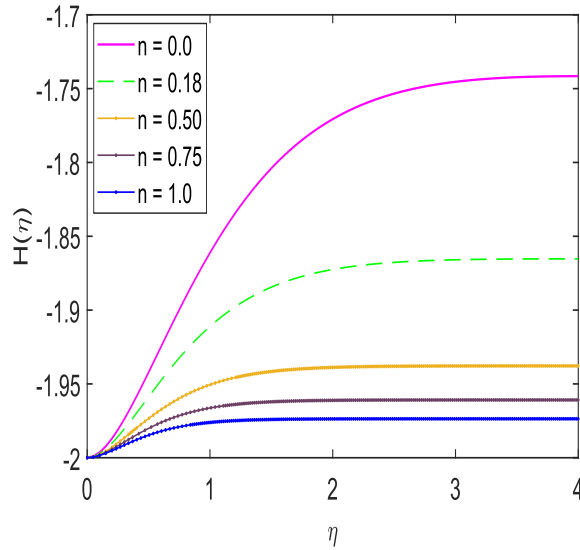
Fig. 2.6: Variation in axial velocity profile $H(\eta)$ with η for different choices of power-law parameter n when $(A = -2.0)$.
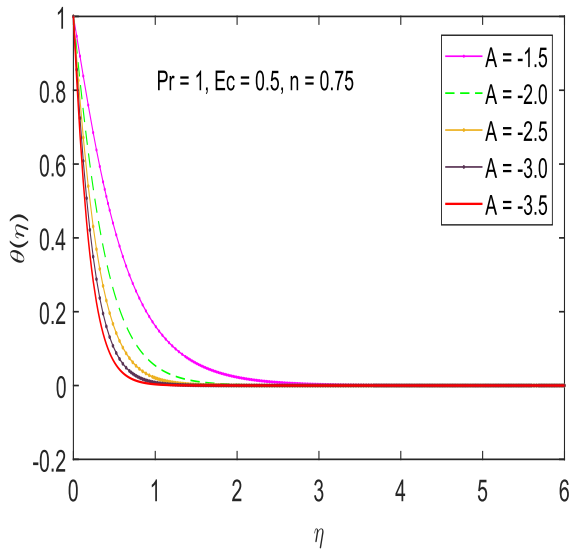
Fig. 2.7: Variation in temperature profile $\theta(\eta)$ with η for different choices of suction parameter *A* in **PST case.**
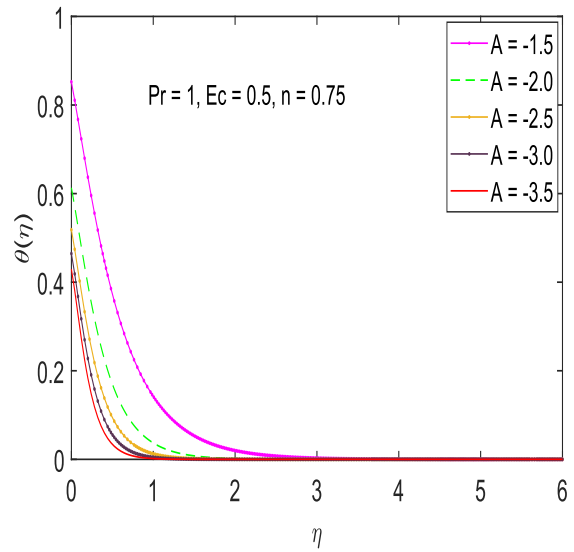
Fig. 2.8: Variation in temperature profile $\theta(\eta)$ with η for different choices of suction parameter *A* in **PHF case.**
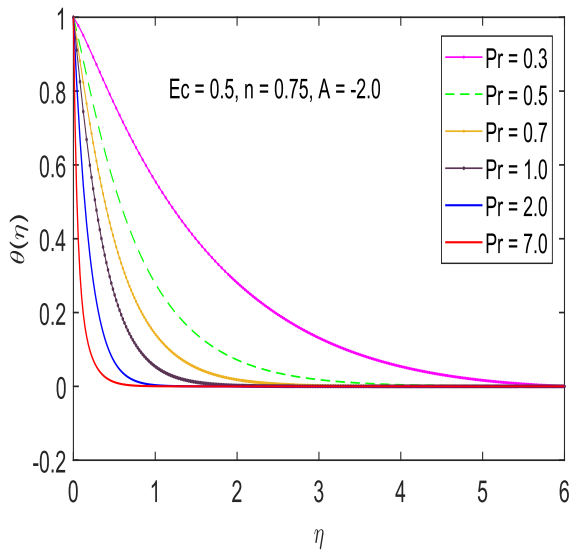
Fig. 2.9: Variation in temperature profile $\theta(\eta)$ with η for different choices of Prandtl number Pr in **PST case.**
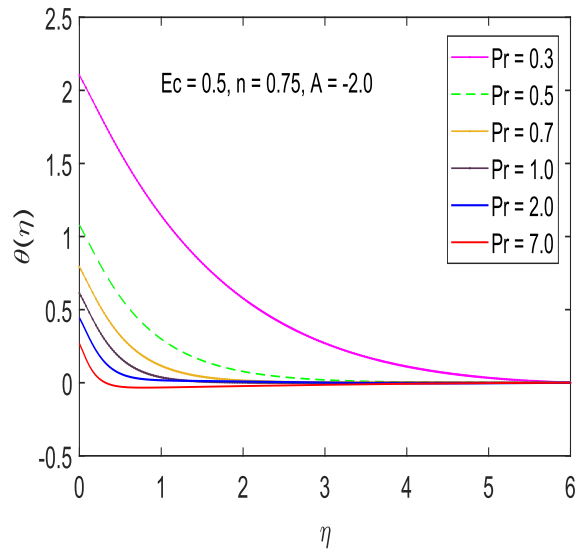
Fig. 2.10: Variation in temperature profile $\theta(\eta)$ with η for different choices of Prandtl number Pr in **PHF case.**
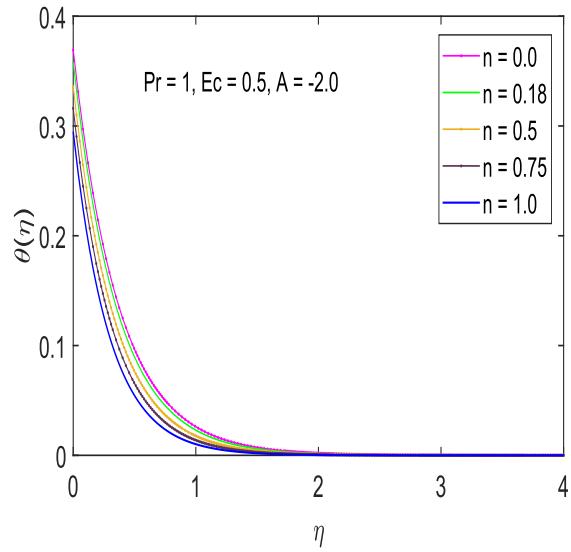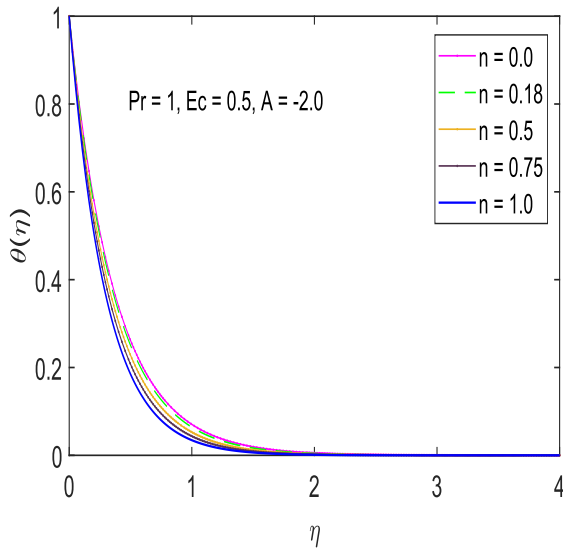
Fig. 2.11: Variation in temperature profile $\theta(\eta)$ with η for different choices of power-law parameter n in **PST case.**

Fig. 2.12: Variation in temperature profile $\theta(\eta)$ with η for different choices of power-law parameter n in **PHF case.**
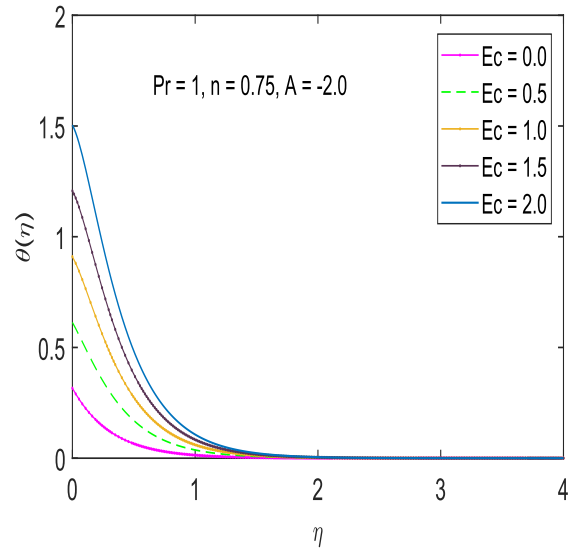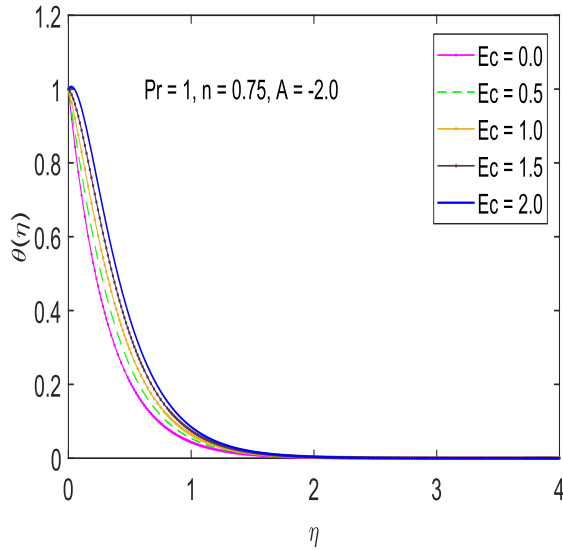
Fig. 2.13: Variation in temperature profile $\theta(\eta)$ with η for different choices of Eckert number Ec in **PST case.**

Fig. 2.14: Variation in temperature profile $\theta(\eta)$ with η for different choices of Eckert number Ec in **PHF case.**

29

Chapter 3

Vortex Flow and Heat Transfer Over a Permeable Disk in the Presence of Concentration Gradient

3.1 Introduction

Concentration gradient effects on the boundary layer formed beneath a vortex flow are formulated in this chapter. Advection-diffusion process is assumed to be influenced by activation energy of chemical reaction; which takes place because fluid media being treated is comprising of chemically reactive substances. Boundary condition for velocity and temperature are similar to those employed in [12]. A dimensional concentration function ϕ is introduced in term of similarity variable η (defined in Chapter 2), which is utilized to obtain self-similar (mass transfer) equation in ϕ. Numerical solution is achieved, which is used to forecast the impacts of chemical reaction and activation energy on the associated mass transport phenomena.

3.2 Problem Formulation

Suppose that fluid media being treated in Chapter 2 contains chemically reactive species. Let C_w and C_∞ be concentrations of species at wall and ambient, respectively. A well-known Arrhenius function is invoked to model energy needed for the activation of chemical reaction.

In view of such assumptions, the problem is governed by the following boundary layer equations:

$$\frac{\partial}{\partial r}(ru) + \frac{\partial}{\partial z}(rw) = 0, \tag{3.1}$$

$$u\frac{\partial u}{\partial r} - \frac{v^2}{r} + w\frac{\partial u}{\partial z} = -\frac{1}{\rho}\frac{\partial p}{\partial r} + \nu\left(\frac{\partial^2 u}{\partial z^2}\right), \tag{3.2}$$

$$\left(u\frac{\partial v}{\partial r} + \frac{uv}{r} + w\frac{\partial v}{\partial z}\right) = \nu\left(\frac{\partial^2 v}{\partial z^2}\right), \tag{3.3}$$

$$\frac{\partial p}{\partial z} = 0, \tag{3.4}$$

$$\rho C_p \left(u \frac{\partial T}{\partial r} + w \frac{\partial T}{\partial z} \right) = k \left(\frac{\partial^2 T}{\partial z^2} \right), \tag{3.5}$$

$$u \frac{\partial C}{\partial r} + w \frac{\partial C}{\partial z} = D \left(\frac{\partial^2 C}{\partial z^2} - k_r^2 \left(\frac{T}{T_\infty} \right)^f e^{-\frac{E_a}{kT}} (C - C_\infty) \right), \tag{3.6}$$

In equation (3.6), the term $k_r^2 (T/T_\infty)^f e^{\frac{-E_a}{kT}}$ is the Arrhenius function in which, $k = 8.61 \times 10^{-5} \, eV/K$ is the Boltzmann constant, f is defined as fitted rate constant which generally lies in the range $-1 < f < 1$, E_a is the activation energy, k_r^2 signifies the reaction rate, C shows the concentration of species and D stands for diffusion coefficient of species.

Boundary conditions are posed as follows:

$$u = 0, \; v = 0, \; w = Av_0 \sqrt{\frac{v}{v_0 r_0}} \left(\frac{r}{r_0} \right)^{n-1} (n+1), \; T = T_w, \; C = C_w \quad \text{at} \quad z = 0,$$

$$u \to 0, \; v \to v_0 \left(\frac{r}{r_0} \right)^{2n-1}, \; T \to T_\infty, \; C \to C_\infty \quad \text{as} \quad z \to \infty, \tag{3.7}$$

3.3 Similarity Solution

For the above generalized boundary conditions, we define following similarity transformations

$$u(r,z) = -v_0 \left(\frac{r}{r_0} \right)^{2n-1} F(\eta),$$

$$v(r,z) = v_0 \left(\frac{r}{r_0} \right)^{2n-1} G(\eta),$$

$$w = Av_0 \sqrt{\frac{v}{v_0 r_0}} \left(\frac{r}{r_0} \right)^{n-1} (n+1) H(\eta) + (n-1)\eta F, \tag{3.8}$$

$$p(r) = \frac{\rho v_0}{4n-2} \left(\frac{r}{r_0} \right)^{4n-2},$$

$$T(r,z) = T_\infty + (T_w - T_\infty)\theta(\eta),$$

$$C(r,z) = C_\infty + (C_w - C_\infty)\phi(\eta),$$

where η is dimensionless similarity variable which is defined as following:

$$\eta = \left(\frac{z}{r_0}\right)\left(\frac{r}{r_0}\right)^{n-1}\sqrt{\frac{v_0 r_0}{v}},$$

(3.9)

By using similarity transformations Eq. (3.6) assumes the following form:

$$-v_0 \left(\frac{r}{r_0}\right)^{2n-1}\left(\frac{z}{r_0}\right)\left(\frac{r}{r_0}\right)^{n-1}\left(\frac{1}{r}\right)\sqrt{\frac{v_0 r_0}{v}}(n-1)F(\eta)\phi'(C_w - C_\infty)$$

$$+ v_0 \left(\frac{r}{r_0}\right)^{2n-1}\left(\frac{1}{r}\right)\sqrt{\frac{v}{v_0 r_0}}[(n+1)H(\eta) + (n-1)\eta F]\phi'\sqrt{\frac{v_0 r_0}{v}}(C_w - C_\infty)$$

$$= \frac{v}{Sc}\left(\frac{1}{r_0}\right)^2\left(\frac{r}{r_0}\right)^{2n-1}\left(\frac{r_0}{r}\right)\frac{v_0 r_0}{v}(C_w - C_\infty)\phi''$$

$$- k_r{}^2(1+\delta\theta)^f \exp(-E/1+\delta\theta)\,(C_w - C_\infty)\phi,$$

where E refers to the non-dimensional activation energy. Further simplification leads to the following:

$$(n+1)H\phi = \frac{1}{Sc}\phi'' - \frac{k_r{}^2}{\frac{v_0}{r}\left(\frac{r}{r_0}\right)^{2n-1}}(1+\delta\theta)^f \exp(-E/1+\delta\theta)\,\phi,$$

(3.10)

By defining the reaction rate $k_r{}^2$:

$$k_r{}^2 = K_r{}^2\left(\frac{v_0}{r}\right)\left(\frac{r}{r_0}\right)^{2n-1}$$

Eq. (3.10) can be cast into the following form:

$$(n+1)H\phi = \frac{1}{Sc}\phi'' - K_r{}^2(1+\delta\theta)^f \exp(-E/1+\delta\theta)\,\phi,$$

(3.11)

By rearraigning the equation, we get:

$$\phi'' = Sc\left[(n+1)H\phi' + K_r{}^2(1+\delta\theta)^f \exp(-E/1+\delta\theta)\,\phi\right],$$

(3.12)

Hence, we are required to solve the following system:

$$H' - F = 0,$$

(3.13)

$$F'' - (n+1)HF' - (1-2n)F^2 - G^2 + 1 = 0,$$

(3.14)

$$G'' - (n+1)HG' + 2nFG = 0,$$

(3.15)

$$\theta'' - \Pr(n+1)H(\eta)\theta' = 0, \tag{3.16}$$

$$\phi'' - Sc\left[(n+1)H\phi' + K_r{}^2(1+\delta\theta)^f \exp(-E/(1+\delta\theta))\,\phi\right] = 0, \tag{3.17}$$

The boundary conditions are following:

$$F(\eta) = 0, \quad G(\eta) = 0, \quad H(\eta) = A, \quad \theta(\eta) = 1, \quad \phi(\eta) = 1 \quad \text{at} \quad \eta = 0,$$
$$F(\eta) \to 0, \quad G(\eta) \to 1, \quad \theta(\eta) \to 0, \quad \phi(\eta) \to 0 \quad \text{as} \quad \eta \to \infty, \tag{3.18}$$

By means of the transformation defined in Eq. (3.8), the PDEs in Eqs. (3.1) − (3.7) transform exactly into a set of coupled non-linear ordinary differential equations (ODEs) subjected to nine suitable boundary conditions in Eq. (3.18).

3.4 Results and Discussions

In table 3.1, wall concentration data is being calculated by varying wall suction parameter A and power-law index parameter n. Originally, wall concentration increases from the solid surface whenever larger suction velocity is accounted. This outcome holds for all considered values of parameter n. Higher values of n, yield higher wall concentration gradient or thinner concentration boundary layer. Moreover, surface concentration is lowered whenever n is decrease.

Table 3.1: Concentration rate $-\phi'(0)$ for differently revolving far-field flow $v \sim r^m$ with the power m in the range from $m = +1$ (solid-body rotation $n = 1$) to $m = -1$ (potential vortex $n = 0$) when $Sc = 1, E = 1, \delta = 0.75, Pr = 1$ and $K_r{}^2 = 1$.

$n \backslash A$	0	-0.42	-0.5	-1.0	-2.0
1.0	NA	1.1478	1.2588	2.1681	4.1115
0.75	NA	1.0708	1.1778	1.9336	3.6249
0.50	NA	0.9881	1.0794	1.7011	3.1418
0.0	NA	0.8550	0.8955	1.1955	2.1868

Concentration profile $\phi(\eta)$ is plotted from the numerical solution for wide range of embedded parameters. Fig. 3.1 includes curves of $\phi(\eta)$ by varying suction-strength parameter A. $\phi(\eta)$ appears to be a monotonically decreasing function of similarity variable η. Moreover, concentration $\phi(\eta)$ appears to be suppressed as suction velocity enlarges. Concentration boundary layer is drastically thinned due to the inclusion of wall suction effect.

To inspect how parameter n influences the concentration boundary layer, Fig. 3.2 is presented which contains graphs of ϕ verses similarity variable η for values of n is the range $0 \leq n \leq 1$. An expansion in concentration boundary layer is detected when the case of potential.

Fig. 3.3 shows the plots of $\phi(\eta)$ as the Schmidt number Sc varies. The effect of Schmidt number is such that $\phi(\eta)$ decreases sharply for growing values of Sc. Physically, for higher Sc-values, mass diffusion coefficient is relatively small and concentration boundary layer is therefore thinner.

Fig. 3.4 presents the concentration profile $\phi(\eta)$ for the different choices of activation energy E. It is clearly visible that activation energy works to increase the value of species concentration in the flow field. The effect of activation energy E on the concentration $\phi(\eta)$ have been shown. It indicates that when the dimensionless activation energy increases, the concentration boundary layer thickens. Because of the low temperature and high activation energy, the reaction rate constant is less and the chemical reaction is slowed.

Fig. 3.5 shows the variation in solute concentration $\phi(\eta)$ by changing temperature difference parameter δ. The solute concentration $\phi(\eta)$ is seen to be a decreasing function of δ. This means that when the temperature difference between the wall and the ambient temperature rises, the thickness of the concentration boundary layer also rises.

Fig. 3.6 is prepared to perceive the importance of reaction rate on concentration $\phi(\eta)$. The reduction in concentration profile $\phi(\eta)$ is accompanied with a large concentration gradient at the wall. Physically, higher values of K_r^2 implies higher destructive chemical reaction rate which in turn reduces the concentration of species and concentration ϕ is therefore seen to be an increasing function of K_r^2.

In Fig. 3.7, the effects of fitted rate constant f on the solute concentration have been shown. It can be observed that an increase in f results in an increase in factor $K_r^2 (1 + \delta\theta)^f \exp(-E/(1 + \delta\theta))$.

This eventually favors the destructive chemical reaction due to which concentration rises. The reduction in ϕ is accompanied with a large concentration gradient at the wall.
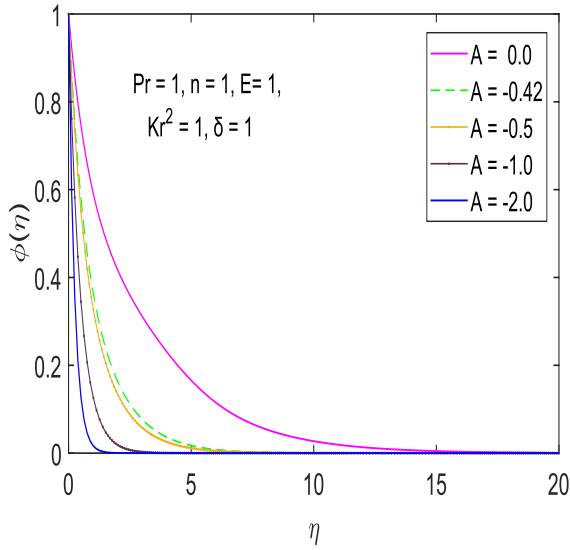
Fig. 3.1: Variation in concentration profile $\phi(\eta)$ with η for different choices of suction parameter A.
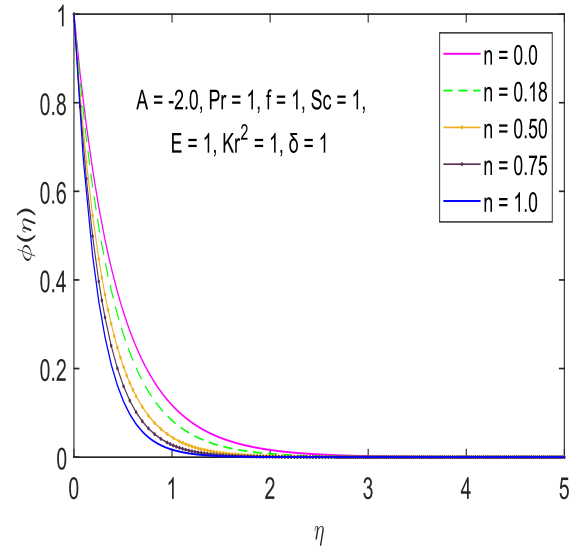
Fig. 3.2: Variation in concentration profile $\phi(\eta)$ with η for different choices of power-law parameter n.
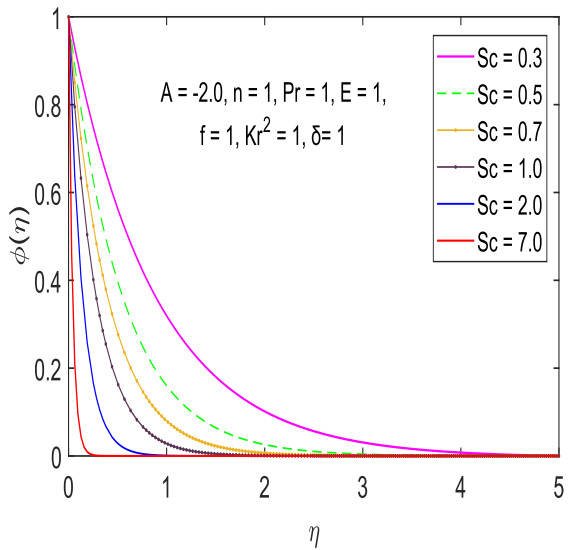
Fig. 3.3: Variation in concentration profile $\phi(\eta)$ with η for different choices of Schmidt number Sc.
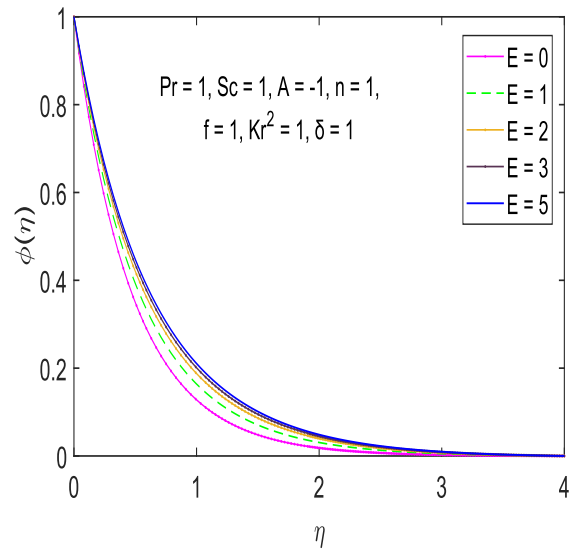
Fig. 3.4: Variation in concentration profile $\phi(\eta)$ with η for different choices of activation energy E.
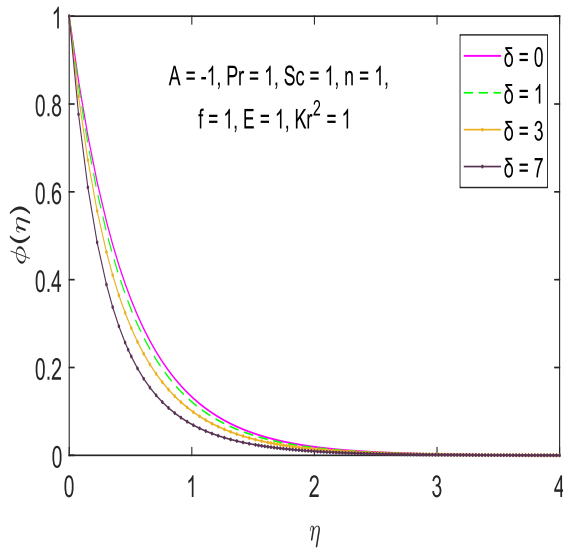
Fig. 3.5: Variation in concentration profile $\phi(\eta)$ with η for different choices of temperature difference parameter δ.
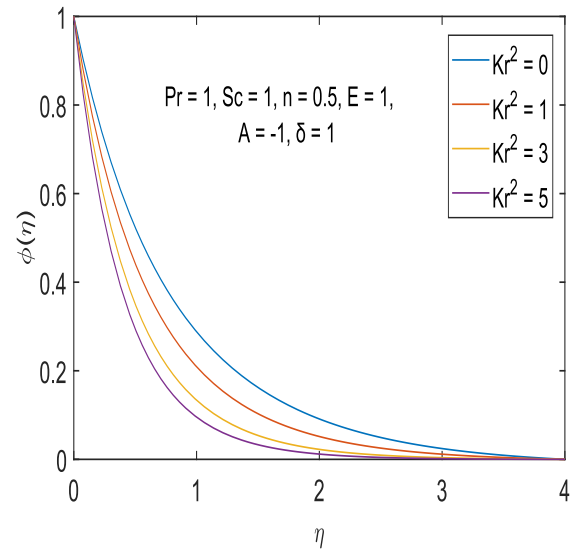
Fig. 3.6: Variation in concentration profile $\phi(\eta)$ with η for different choices of reaction rate parameter $K_r{}^2$.
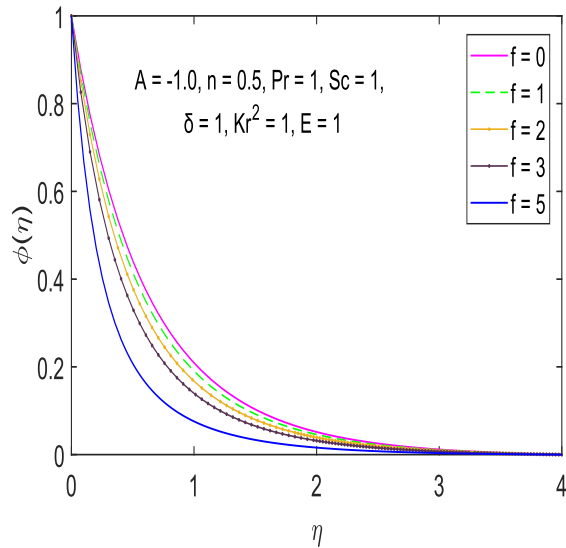
Fig. 3.7: Variation in concentration profile $\phi(\eta)$ with η for different choices of fitted rate constant f.

Chapter 4

Conclusions

Heat and mass transport phenomena in a boundary layer formed under a generalized vortex flow are investigated. Generalized vortex flow is characterized by a power-law tangential velocity. Heat transport problem is solved in the existence of viscous dissipation term for two different kinds of boundary conditions. Furthermore, mass transport phenomena is analyzed by incorporating activation energy term. Main conclusions of the problem are listed below:

- Energy equation with viscous dissipation term is solved by assuming two different thermal boundary conditions. The influence of viscous dissipation term is such that heat generation enhances for increasing frictional heating effect which leads to an enhanced temperature profile.

- Governing problem is self-similar only if surface temperature and surface heat flux are prescribed as $T_w = T_\infty + T_0(r/r_0)^{4n-2}$ and $q_w = D(r/r_0)^{5n-3}$ respectively. Otherwise, the problem is locally similar.

- Meaningful solutions of the energy and concentration equations are possible only when the axial flow is directed downward. This can be ensured by considering sufficiently large value of wall suction parameter A.

- Activation energy of chemical reaction and concentration profile are directly related with each other. Moreover, higher the rate of chemical reaction, smaller will be the concentration boundary layer thickness.

- Suction phenomena plays an important role in enhancing heat transfer from the disk in case of prescribed wall temperature.

- Power-law index n has only a marginal influence on thermal and solute boundary layers. Values of temperature and concentration functions in a potential vortex case $(n = 0)$ are lesser than that in the case of rigid body rotation $(n = 1)$.

Bibliography

[1]   M. Menzinger and Re Wolfgang, The meaning and use of the Arrhenius activation energy, Angewandte Chemie Int. Edit. in Eng. 8 (1969) 438-444.

[2]   T. V. Kármán, Über laminare und turbulente Reibung, ZAMM-J. Appl. Math. & Mech. 1 (1921) 233-252.

[3]   U. T. Bödewadt, Die Drehströmung über festem Grunde, ZAMM-J. Appl. Math. & Mech. 20 (1940) 241-253.

[4]   G. K. Batchelor, Note on the class of the solutions of the Navier-Stokes equations representing steady non- rotationally symmetric flow, Quart. J. Appl. Math. 4 (1951) 29-41.

[5]   B. Sahoo, Effects of slip on steady Bödewadt flow and heat transfer of an electrically conducting non-Newtonian fluid, Commun. Nonlinear Sci. & Numer. Simulat. 16 (2011) 4284-4295.

[6]   B. Sahoo, Steady Bödewadt flow of a Non-Newtonian Reiner-Rivlin Fluid, Diff. Eqs. & Dynam. Syst. 20 (2012) 367-376.

[7]   M. Turkyilmazoglu, Bödewadt flow and heat transfer over a stretching stationary disk, Int. J. Mech. Sci. 90 (2015) 246-250.

[8]   P. T. Griffiths, S. J. Garrett, S. O. Stephen and Z. Hussain, Quantifying non-Newtonian effects in rotating boundary-layer flows, European J. Mech. –B/Fluids. 61 (2017) 304-309.

[9]   V. K. Joshi, P. Ram, R. K. Sharma and D. Tripathi, Porosity effect on the boundary layer Bödewadt flow of a magnetic nanofluid in the presence of geothermal viscosity, European Phys. J. Plus. 132 (2017) Article ID:254.

[10]   G. Nath and B. J. Venkatachala, The effect of suction on boundary layer for rotating flows with or without magnetic field, Proc. Indian Acad. Sci. 85 (1977) 332–337.

[11]   M. Rahman and H. I. Andersson, On heat transfer in Bödewadt flow, Int. J. Heat & Mass Transf. 112 (2017) 1057–1061.

[12]   M. Rahman and H. I. Andersson, Heat transfer in generalized vortex flow over a permeable surface, Int. J. Heat and Mass Transf. 118 (2018) 1090-1097.

[13]   A. J. Chamkha, A. M. Rashad, H. Al-Mudhaf, Heat and mass transfer from truncated cones with variable wall temperature and concentration in the presence of chemical reaction effects, Int. J. Numer. Meth. Heat & Fluid Flow 22 (2012) 357–376.

[14]   B. Mallikarjuna, A. M. Rashad, A. J. Chamkha and S. H. Raju, Chemical reaction effects on MHD convective heat and mass transfer flow past a rotating vertical cone embedded in a variable porosity regime, Afrika Matematika. 27 (2015) 645–665.

[15]   C. Zhang, L. Zheng, X. Zhang and G. Chen, MHD flow and radiation heat transfer of nanofluids in porous media with variable surface heat flux and chemical reaction, Appl. Math. Modell. 39 (2015) 165–181.

[16]   N. Khan, T. Mahmood, M. Sajid, M.S. Hashmi, Heat and mass transfer on MHD mixed convection axisymmetric chemically reactive flow of Maxwell fluid driven by exothermal and isothermal stretching disks, Int. J. Heat Mass Transf. 92 (2016) 1090–105.

[17] F. Mabood, S. Shateyi, M. M. Rashidi, E. Momoniat and N. Freidoonimehr, MHD stagnation point flow heat and mass transfer of nanofluids in porous medium with radiation, viscous dissipation and chemical reaction. Adv. Powder Technol. 27 (2016) 742–749.

[18] S. U. Jan, S. U. Haq, S. I. A. Shah, and I. Khan, Heat and mass transfer of free convection flow over a vertical plate with chemical reaction under wall–slip effect, Arabian J. Sci. & Eng. 44 (2019) 9869-9887.

[19] T. Zhao, M. R. Khan, Y. Chu, A. Issakhov, R. Ali, and S. Khan, Entropy generation approach with heat and mass transfer in magnetohydrodynamic stagnation point flow of a tangent hyperbolic nanofluid, Appl. Math. & Mech. 42 (2021) 1205-1218.

[20] A. R. Bestman, Natural convection boundary layer with suction and mass transfer in a porous medium, Int. J. Eng. Res. 14 (1990) 389–396.

[21] V. M. Soundalgekar, Free convection effects on the stokes problem for infinite vertical plate, ASME J. Heat Transf. 99 (1977) 499-501.

[22] U. N. Das, R. Deka and V. M. Soundalgekar, Effects of mass transfer on flow past an impulsively started infinite vertical plate with constant heat flux and chemical reaction, Forschung im Ingenieurwesen 60 (1994) 284-287.

[23] M. Dhlamini, P. K. Kameswaran, P. Sibanda, S. Motsa and H. Mondal, Activation energy and binary chemical reaction effects in mixed convective nanofluid flow with convective boundary conditions, J. Comput. Design & Eng. 6 (2019) 149-158.

[24]   M. Khan, A. Hafeez and J. Ahmed, Impacts of non-linear radiation and activation energy on the axisymmetric rotating flow of Oldroyd-B fluid, Physica A: Stat. Mech. & Applicat. 580 (2021) Article ID:124085.

[25]   Abbas, S. Zaheer, M. I. Khan, S. Kadry, W. A. Khan, M. I. U. Rehman and M. Waqas, Fully developed entropy optimized second order velocity slip MHD nanofluid flow with activation energy, Comput. meth. & prog. biomed. 190 (2020) Article ID:105362.

[26]   S. Tahira, M. Mustafa, and A. Mushtaq, Rotationally symmetric flow of Cu-Al2O3/water hybrid nanofluid over a heated porous boundary, Proceedings of the Inst. of Mech. Eng., Part C: J. Mech. Eng. Sci. (2021) doi.org/10.1177/09544062211023104.